AJNR

Hemodynamic Characteristics in Ruptured and Unruptured Intracranial Aneurysms: A Prospective Cohort Study Utilizing the AneurysmFlow Tool

Dang Luu Vu, Van Hoang Nguyen, Huu An Nguyen, Quang Anh Nguyen, Anh Tuan Tran, Hoang Kien Le, Tat Thien Nguyen, Thu Trang Nguyen, Cuong Tran, Xuan Bach Tran, Chi Cong Le and Laurent Pierot

AJNR Am J Neuroradiol 2025, 46 (1) 75-83
doi: https://doi.org/10.3174/ajnr.A8444
http://www.ajnr.org/content/46/1/75

Hemodynamic Characteristics in Ruptured and Unruptured Intracranial Aneurysms: A Prospective Cohort Study Utilizing the AneurysmFlow Tool

Dang Luu Vu, Van Hoang Nguyen, Huu An Nguyen, Quang Anh Nguyen, Anh Tuan Tran, Hoang Kien Le, Tat Thien Nguyen, Thu Trang Nguyen, Cuong Tran, Xuan Bach Tran, Chi Cong Le, and Laurent Pierot

ABSTRACT

BACKGROUND AND PURPOSE: Hemodynamic factors significantly influence the onset, progression, and rupture of intracranial aneurysms (IAs). Current rupture risk prediction scores focus primarily on the clinical, anatomic, and morphologic aspects. This study aimed to investigate the hemodynamic characteristics differences between ruptured and unruptured IAs.

MATERIALS AND METHODS: Conducted from July 2021 to July 2022, this prospective cohort study involved patients with ruptured and unruptured IAs undergoing DSA. Hemodynamic characteristics were assessed by using the AneurysmFlow tool. Hemodynamic, clinical, anatomic, and morphologic parameters were compared between ruptured and unruptured IA groups.

RESULTS: The study included 127 patients with 135 aneurysms (67 ruptured, 68 unruptured). Complex flow patterns (type 3 and 4) were observed more frequently in ruptured aneurysms compared with unruptured aneurysms (OR, 5.57; 95% CI, 2.49–12.45; $P < .001$) in univariate analysis, and were also more common in unruptured aneurysms associated with daughter sac features ($P = .015$). The mean aneurysm flow amplitude (MAFA) was lower in ruptured aneurysms, and associated with lower flow velocity in the parent artery related to vasospasm. MAFA in the aneurysmal dome or any additional daughter sacs was lowest compared with other regions inside the aneurysms. The technical failure rate of AneurysmFlow measurements was 8.5% (12 of 139 patients). Additionally, hypertension (OR, 0.42; 95% CI, 0.30–0.54; $P < .001$), bifurcation location (anterior communicating artery/anterior cerebral artery/MCA/posterior communicating artery/posterior circulation) (OR, 0.17; 95% CI, 0.05–0.29; $P = .005$), and irregular shape (OR, 0.19; 95% CI, 0.05–0.35; $P = .012$) were identified as independently associated with rupture.

CONCLUSIONS: Complex flow patterns identified on the AneurysmFlow tool are significantly more common in ruptured and unruptured aneurysms associated with daughter sac features. The lowest MAFA in the aneurysmal dome and daughter sacs likely indicates specific pathophysiologic changes within the aneurysm wall associated with rupture incidence. Hypertension, bifurcation location, and an irregular shape are independently associated with the risk of rupture. Further multicenter studies with larger sample sizes are needed to validate these findings.

ABBREVIATIONS: ACA = anterior cerebral artery; AcomA = anterior communicating artery; CFD = computational fluid dynamics; IA = intracranial aneurysm; MAFA = mean aneurysm flow amplitude; PcomA = posterior communicating artery

SAH caused by the rupture of an intracranial aneurysm (IA) remains a devastating condition with high mortality and morbidity despite remarkable advancements in surgical and endovascular treatments.[1,2] Numerous studies have focused on identifying the clinical, anatomic, and morphologic factors affecting the rupture risk of unruptured IA,[3-9] leading to the development of various scoring systems to predict this risk.[10-12] However, a crucial aspect that remains underexplored in these scoring systems are certain hemodynamic factors, which are pivotal in the initiation, progression, and rupture of IAs.[13] In recent years, computational fluid dynamics (CFD) methodologies have been applied across various domains, including the study of cerebral aneurysms by using patient-specific geometric models since 2003.[14] These studies have shown that hemodynamics play an important role in understanding aneurysm pathology.[15-26]

Received June 3, 2024; accepted after revision July 22.

From the Radiology Center (D.L.V., V.H.N., H.A.N., Q.A.N, A.T.T., H.K.L., Tat T.N., Thu T.N., C.T., X.B.T., C.C.L.), Bach Mai Hospital, Hanoi, Vietnam; Department of Radiology (D.L.V., Q.A.N.), Hanoi Medical University, Hanoi, Vietnam; Department of Neuroradiology (H.A.N., L.P.), Hôpital Maison-Blanche, Université Reims-Champagne-Ardenne, Reims, France; Stroke and Cerebrovascular Disease Department (A.T.T.), and Radiology Department (A.T.T.), University of Medicine and Pharmacy, Vietnam National University, Hanoi, Vietnam.

Please address correspondence to Huu An Nguyen, Bach Mai Hospital–Radiology, No 78, Giai Phong St, Dong Da District, Hanoi 100000, Viet Nam; e-mail: nguyenhuuan.dr@gmail.com

Indicates article with online supplemental data.

http://dx.doi.org/10.3174/ajnr.A8444

SUMMARY

PREVIOUS LITERATURE: Numerous studies have focused on identifying the clinical, anatomic, and morphologic factors affecting the rupture risk of unruptured intracranial aneurysms, leading to the development of various scoring systems to predict this risk, including the Practical Risk Score (PHASES), the Earlier Subarachnoid Hemorrhage, Location of the Aneurysm, Age >60 years, Population, Size of the Aneurysm, and Shape of the Aneurysm (ELAPSS) score, and the UIA Treatment Score (UIATS) consensus. However, a crucial aspect that remains underexplored in these scoring systems is certain hemodynamic factors, which are pivotal in the initiation, progression, and rupture of intracranial aneurysms.

KEY FINDINGS: Complex flow patterns, identified with the AneurysmFlow tool, are common in ruptured aneurysms and those with daughter sacs. Lowest MAFA in the dome and daughter sacs indicates pathophysiologic changes linked to rupture. Hypertension, bifurcation location, and irregular shape of unruptured IA are also confirmed as independent rupture risk factors.

KNOWLEDGE ADVANCEMENT: Complex flow patterns in intracranial aneurysms, identified via DSA-based flow quantification, are more frequent in ruptured aneurysms and unruptured aneurysms with daughter sacs. The lowest MAFA in the dome and daughter sacs indicates specific pathophysiologic changes associated with aneurysm rupture.

Unlike image-based, patient-specific computational models used in CFD, blood velocity can be quantified by using a DSA-based flow quantification algorithm. This algorithm estimates blood velocity based on the spatiotemporal intensity changes of iodinated contrast wavefronts, providing results almost instantaneously,[27,28] unlike the theoretical delay of hours or more typically associated with CFD methods. This quick accessibility is beneficial, particularly if analyzing changes in flow conditions after neurointerventions.[28,29]

The AneurysmFlow tool, developed by Phillips Healthcare, is a unique DSA-based flow quantification tool designed specifically for neurointerventional procedures. It measures blood flow vectors and velocities by injecting contrast material into the bloodstream, which is then modulated by the cardiac cycle and detected in the x-ray signal. Although a few studies have used this tool to evaluate the effectiveness of endovascular interventions,[28,29] to our knowledge, no studies have yet reported its use to assess aneurysm rupture risk. Therefore, this study aims to identify differences in aneurysm flow characteristics between ruptured and unruptured IAs by using the AneurysmFlow tool, alongside clinical, anatomic, and morphologic characteristics.

MATERIALS AND METHODS

Study Design

This prospective, single-center cohort study was conducted from July 2021 to July 2022 and included 127 patients. Approval was obtained from the institutional review board or ethics committee, and informed consent was obtained from all participating patients or their legal representatives. The study adhered to the Strengthening the Reporting of Observational Studies in Epidemiology checklist to ensure rigorous and transparent reporting (Online Supplemental Data).

Patient Selection

In this study, patients were included based on the following criteria: 1) age older than 18 years, 2) rupture status according to previous CTA/MRA imaging, 3) confirmation of IA presence through DSA, and 4) use of the AneurysmFlow tool to assess hemodynamic characteristics within the aneurysms.

Exclusion criteria were as follows: 1) patients with severe renal failure or allergies to contrast agents, 2) patients for whom hemodynamic measurement by using the AneurysmFlow tool was unsuccessful or for whom insufficient information was collected in the study, and 3) patients who declined to participate in the study.

Aneurysm Flow Evaluation Procedure

Cerebral angiograms were conducted via standard transfemoral catheterizations. DSA-based aneurysm flow quantification was carried out by using the DSA biplane system (Azurion 7 B20/15, Philips Healthcare). A 5F/0.038-inch catheter (JB2; MicroVention) was placed in the cervical segment of the ICA or the V2 segment of the vertebral artery. A 3D rotational angiography then identified the optimal projection angle of the aneurysm neck for the 2D flow sequence, avoiding vessel overlap and providing optimal vessel geometry for quantitative volumetric blood flow measurements. Subsequently, a high-speed 2D DSA run (60 frames per second) was performed with a standardized injection duration of 4 seconds at a rate of 1.5 mL/s by using an iohexol contrast agent (Omipaque 300; GE Healthcare). The injection was administered via an angiographic contrast injector (Illumina Neo; Liebel-Flarsheim) under 350 psi pressure. The aneurysm flow data were seamlessly integrated into the AneurysmFlow software within the advanced Philips Healthcare interventional workstation for processing and analysis, which included parent artery segmentation, aneurysm segmentation, ROI selection, and flow measurements.[30]

Classification of Flow Patterns within the Aneurysm

Following Cebral et al,[20] we classified flow patterns within the aneurysm by using the AneurysmFlow tool into 4 types (Fig 1):

- Type 1: Constant flow direction with a single vortex. Blood flows consistently from the parent artery through the inflow, dome, and outflow regions, forming a single stable vortex within the aneurysm throughout the cardiac cycle.

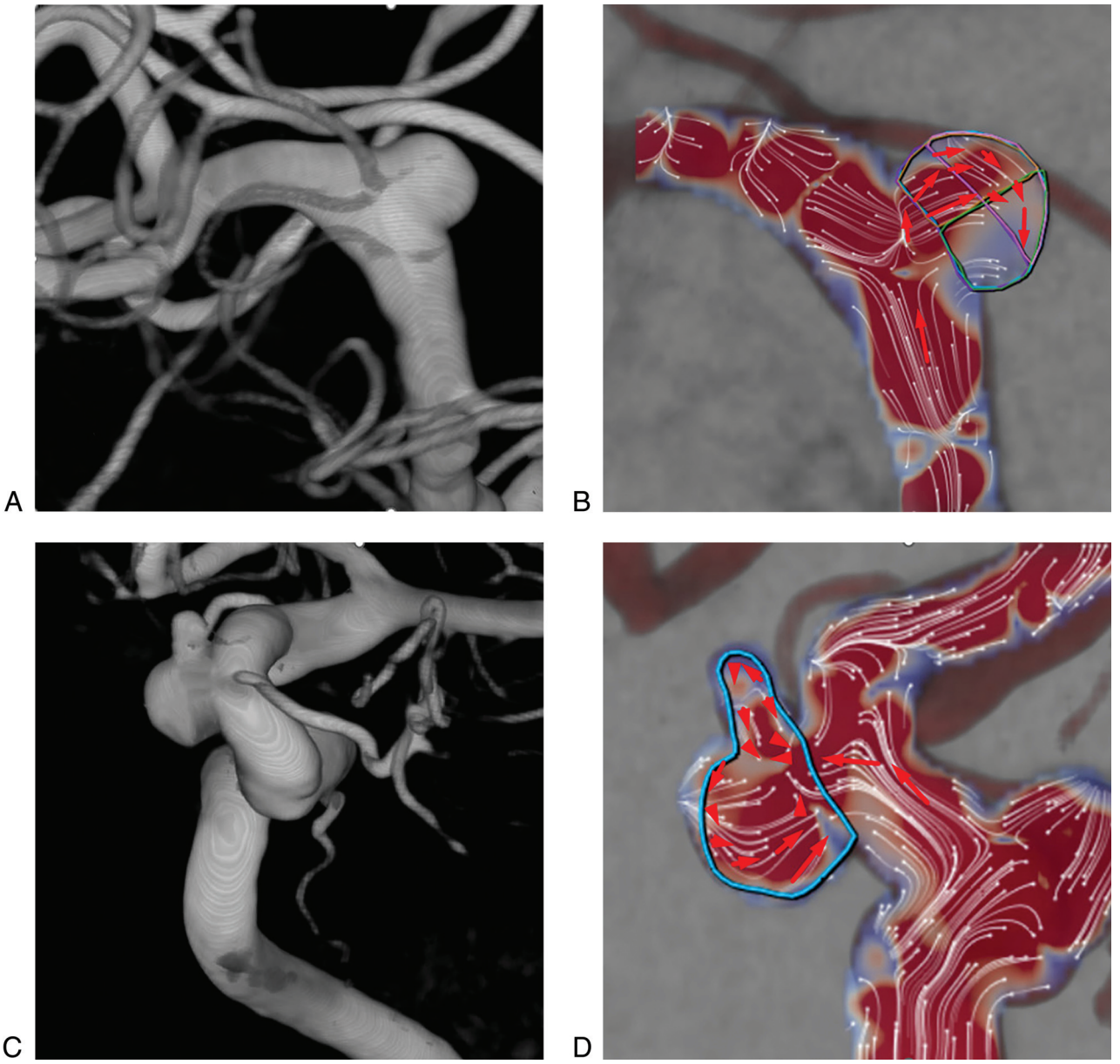

FIG 1. Four types of aneurysm flow patterns inside the aneurysm by using the AneurysmFlow tool. Type 1 of aneurysm flow pattern: 3D-DSA (*A*) and AneurysmFlow tool result (*B*) of an MCA aneurysm demonstrated constant flow direction with a single vortex. Type 2 of aneurysm flow pattern: 3D-DSA (*C*) and AneurysmFlow tool result (*D*) of an ophthalmic ICA aneurysm demonstrated constant flow direction with multiple vortices. Type 3 of aneurysm flow pattern: 3D-DSA (*E*) and AneurysmFlow tool result (*F*) of an MCA aneurysm demonstrated changing flow direction with a single vortex. Type 4 of aneurysm flow pattern: 3D-DSA (*G*) and AneurysmFlow tool result (*H*) of a PcomA aneurysm demonstrated changing flow direction with multiple vortices.

- Type 2: Constant flow direction with multiple vortices, unchanged during the cardiac cycle. Blood flows steadily in 1 direction, creating several stable vortices that remain unchanged in number and position throughout the cardiac cycle.
- Type 3: Changing flow direction creating a single vortex. Blood flow varies during the cardiac cycle, resulting in a single vortex that may move or shift with the changing flow.
- Type 4: Changing flow direction resulting in the creation or destruction of multiple vortices. Blood flow direction changes throughout the cardiac cycle, leading to the dynamic formation and dissipation of multiple vortices.

Quantification of Mean Aneurysm Flow Amplitude

To gain a detailed understanding of the mean aneurysm flow amplitude (MAFA) within the aneurysm, measurements were taken at 4 distinct locations: the neck region, inflow region, dome region, and outflow region. Four smaller ROIs with approximately the same measuring area were placed at these locations, representing the MAFA at each respective site (Fig 2). Where feasible, the MAFA within the daughter sac of the aneurysm was assessed (Fig 3).

Potential Confounders

For patients receiving intervention treatment during the same session as AneurysmFlow imaging, general anesthesia could be used.

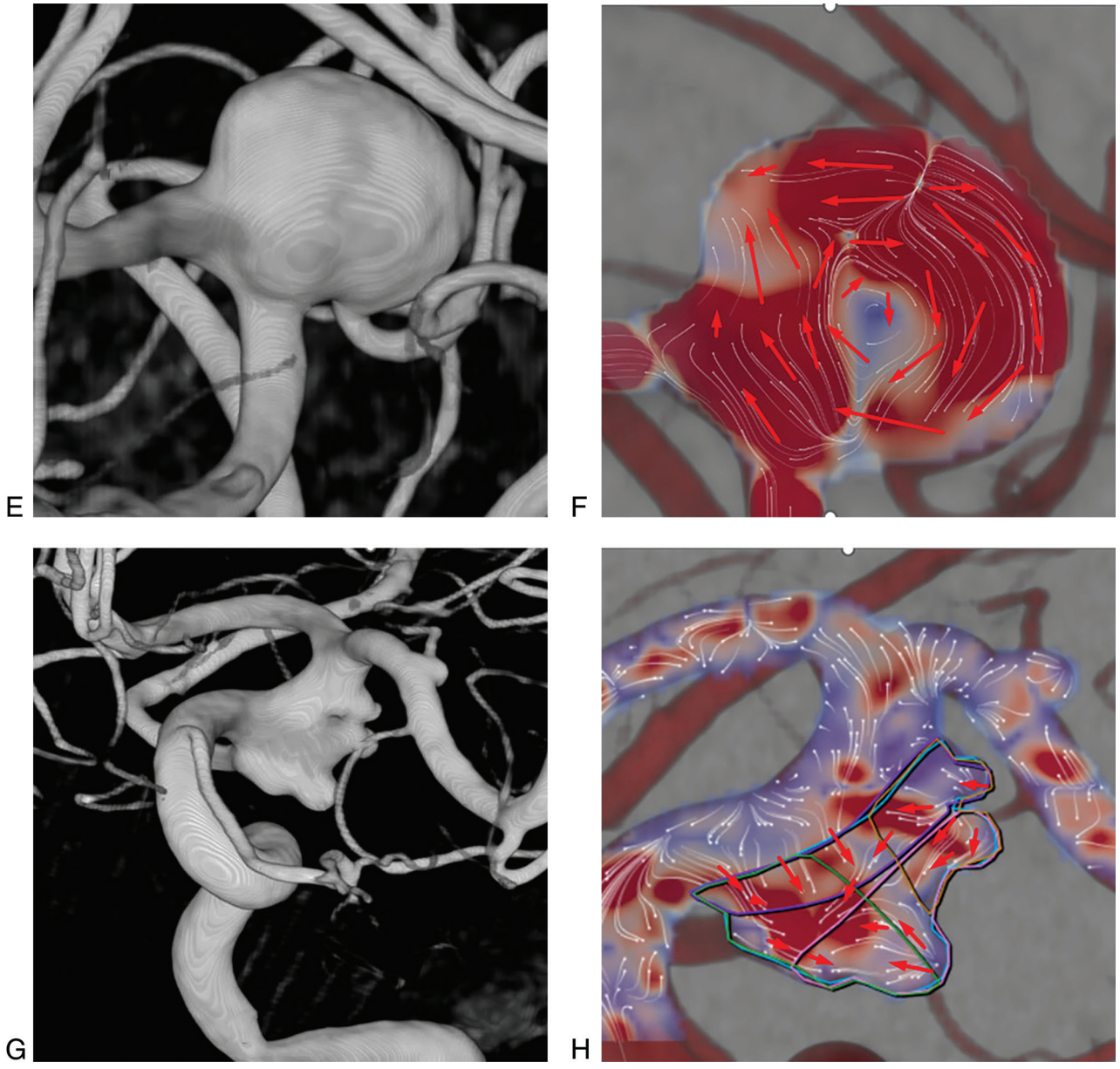

FIG 1. Continued.

To prevent thromboembolic complications, all patients received a 2500 IU intra-arterial heparin bolus after femoral puncture. For unruptured wide-necked aneurysms requiring pretreatment dual antiplatelet therapy for diagnostic angiography and endovascular treatment in the same session, patients received clopidogrel 75 mg/d and aspirin 81 mg/d for 5 days.

Outcome Measurement

For patients receiving intervention treatment after AneurysmFlow imaging, clinical and imaging outcomes were evaluated by using the mRS at a scheduled 3-month posttreatment visit or via telephone. For unruptured aneurysms under follow-up management, clinical and imaging outcomes were assessed at regular intervals.

Data Collection

Collected patient data included: age, sex, hypertension status (defined as systolic blood pressure >140 mm Hg or diastolic blood pressure >90 mm Hg or use of antihypertensive medications), smoking status, prior history and date of SAH occurrence, total number of IAs, aneurysm location and diameter, characteristics of aneurysm shape (regular/irregular, presence of additional daughter sac), hemodynamic characteristics assessed by using the AneurysmFlow tool, type of management, and the mRS at 3 months.

Statistical Analysis

Continuous variables were reported by using medians and interquartile ranges (IQR), while categoric variables were presented as percentages. The Student *t* test was used for continuous variables and the Mann-Whitney *U* test or χ^2 test was used for categoric variables. Univariate and multivariate logistic regression analyses were conducted to determine the OR for associations between prognostic factors and the rupture status.

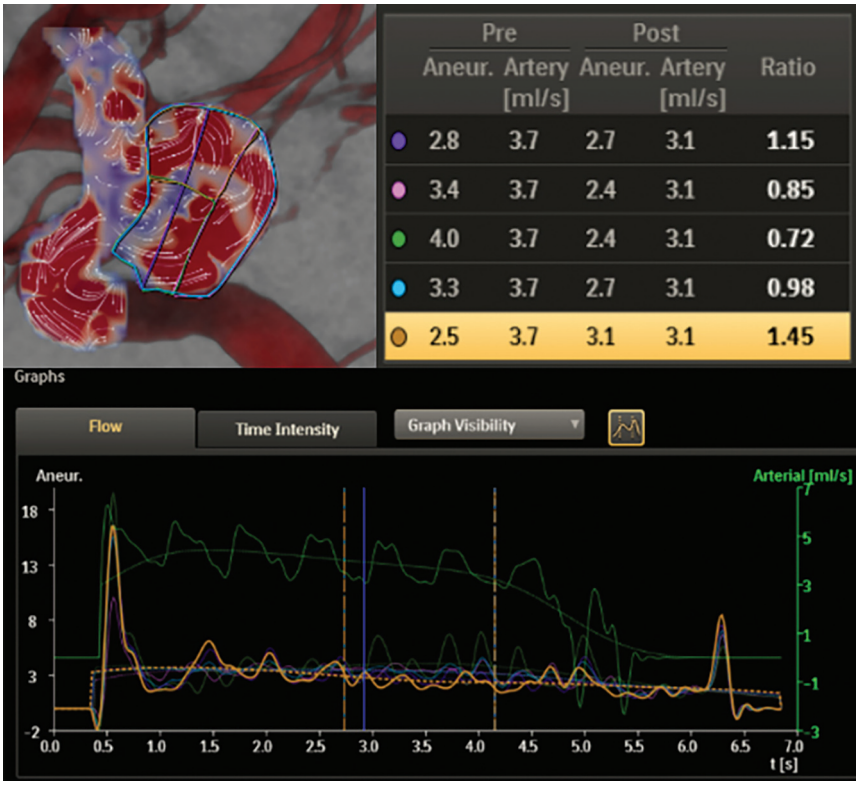

FIG 2. Measurement of MAFA on the AneurysmFlow Tool. Measurement of the MAFA of the entire aneurysm (*ROIs in turquoise*). Measurement of the MAFA of the neck region of the aneurysm (*ROIs in violet*). Measurement of the MAFA of the inflow region of the aneurysm (*ROIs in light brown*). Measurement of the MAFA of the dome region of the aneurysm (*ROIs in pink*). Measurement of the MAFA of the outflow region of the aneurysm (*ROIs in bright green*).

A subgroup analysis of unruptured aneurysms was performed based on 2 models of flow patterns: complex flow pattern (type 3 and 4) and simple flow pattern (type 1 and 2).

A P value $\leq .05$ was considered statistically significant difference for a 95% CI. Data were processed and analyzed by using SPSS software (version 16.0; SPSS).

RESULTS

Unsuccessful Rate of AneurysmFlow Tool

From July 2021 to July 2022, 230 patients with IAs were treated at our neurointerventional center. Among them, 139 patients underwent evaluation of aneurysm flow characteristics, but in 12 patients (8.6%), the AneurysmFlow tool was unsuccessful. The failures were attributed to the small size of the aneurysms (aneurysm width and aneurysm height <4 mm), the contrast medium arriving slower than the start of DSA acquisition, a field of view exceeding manufacturer recommendations (>22 cm), overlap of the parent artery or other branches on the aneurysm region, or distal aneurysms (in the anterior communicating artery [AcomA] location) preventing parent artery segmentation. Ultimately, 127 patients with 135 aneurysms (67 ruptured and 68 unruptured) were eligible for the assessment of hemodynamic characteristics by using AneurysmFlow tool and were included in the study.

Patient Characteristics and Outcomes

Sixty-three percent were female patients (80 of 127), with a female-to-male ratio of 1:7. The median age was 57 years (IQR, 49–66, range 27–84 years). The most common aneurysm location was the ICA (59 aneurysms, 22.7%), followed by the posterior communicating artery (PcomA) (31 aneurysms, 11.9%), AcomA (30 aneurysms, 11.5%), MCA (10 aneurysms, 3.8%), anterior cerebral artery (ACA) (2 aneurysms, 0.8%), basilar artery (2 aneurysms, 0.8%), and vertebral artery (1 aneurysm, 0.4%). One hundred two IAs were characterized as small (< 7 mm, 75.6%). Medium-sized aneurysms (7–9.9 mm) were observed in 22 cases (16.3%), while large aneurysms (10–19.9 mm) were found in 11 cases (8.1%).

In the ruptured aneurysm group, CTA was the primary diagnostic tool, used in 97% of all cases (65 of 67), with MRA used in the remaining 2 cases. DSA was performed after the rupture of aneurysms. Most ruptured aneurysms (65 of 67, 97%) were evaluated for AneurysmFlow imaging on the first day, while the remaining 2 cases were assessed on the second day after rupture. The most common location was the AcomA (29 of 67 cases, 43.3%), followed by the PcomA (19 cases, 28.4%), ICA (10 cases, 14.9%), MCA (7 cases, 10.4%), ACA (1 case, 1.5%), and the posterior circulation (1 case, 1.5%). Most ruptured aneurysms were small (<7 mm) (50 of 67 cases, 75%). All 67 patients with ruptured IAs underwent emergency coil treatment with coils alone in 49 cases (73.1%) and balloon-assisted coiling in 18 cases (26.9%). At the 3-month follow-up, 63 patients (94%) had no neurologic deficit (mRS 0), 2 showed a mild deficit (mRS 1), and 2 patients had died (3%).

In the unruptured aneurysm group, most were located in the ICA (49 of 68 cases, 72.1%), followed by the PcomA (12 cases, 17.6%), MCA (3 cases, 4.4%), posterior circulation (2 cases, 3.0%), AcomA (1 case, 1.5%), and ACA (1 case, 1.5%). Of these 68 unruptured aneurysms, 61 cases (89.7%) received interventional treatment: 52 with flow diverter stents (76.5%), 6 with balloon-assisted coiling (8.8%), 2 with Woven EndoBridge (MicroVention, Tustin, CA) devices (2.9%), and 1 with coils alone (1.5%). The remaining 7 aneurysms (10.3%), all small (<5 mm) and regularly shaped in the ICA, were monitored. Clinical outcomes in the treatment group showed no neurologic deficit in 57 of 61 cases (93.4%), mild disability (mRS 3) in 3 cases (4.9%), and 1 death (1.6%) at 3 months. No ruptures were observed in the monitored group during the long-term follow-up.

Comparing Hemodynamic, Clinical, Anatomic, and Morphologic Characteristics of Ruptured and Unruptured Aneurysms

Online Supplemental Data show statistically significant differences in flow patterns, MAFA within the aneurysm, flow velocity of

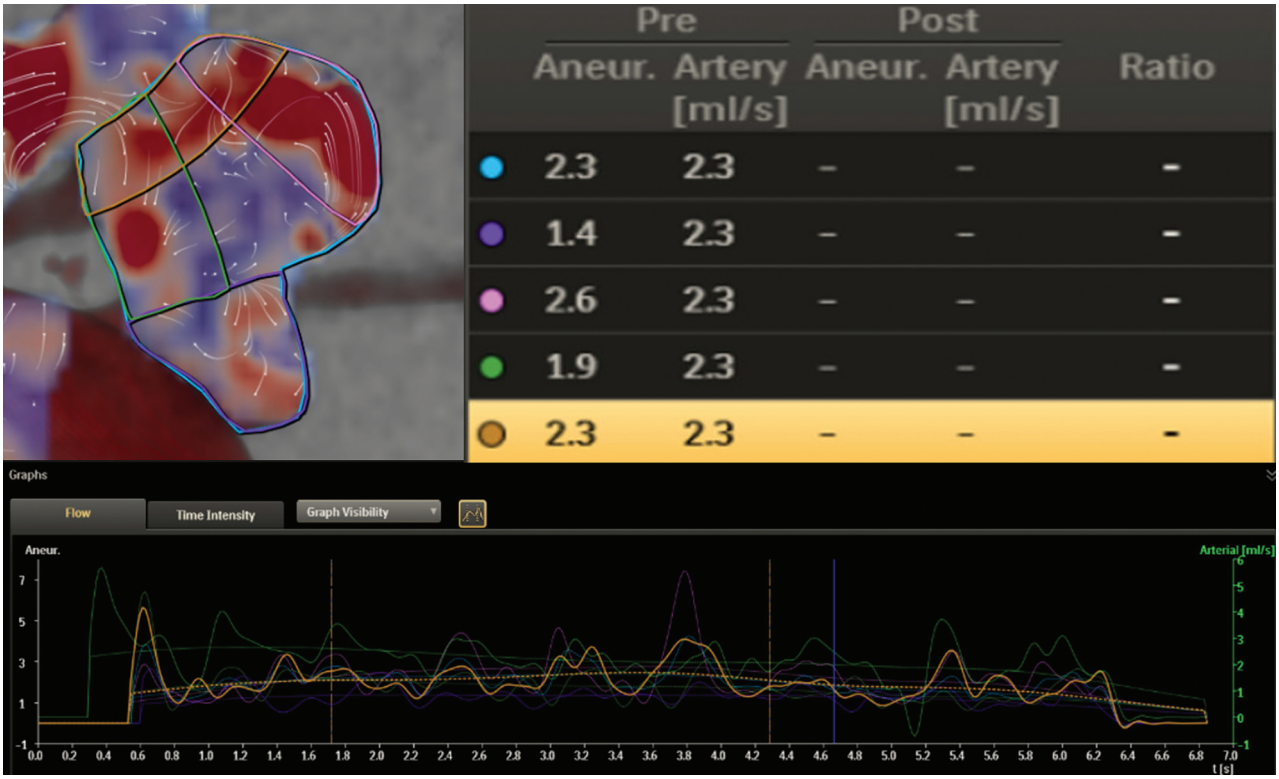

FIG 3. Measurement of MAFA of the daughter sac of the aneurysm on the AneurysmFlow Tool. Measurement of the MAFA of the entire aneurysm (*ROIs in turquoise*). Measurement of the MAFA of the daughter sac of the aneurysm (*ROIs in violet*). Measurement of the MAFA of the inflow region of the aneurysm (*ROIs in pink*). Measurement of the MAFA of the neck region of the aneurysm (*ROIs in light brown*). Measurement of the MAFA of the outflow region of the aneurysm (*ROIs in bright green*).

the parent artery, hypertension, aneurysm location, sac width, neck width, aspect ratio, and aneurysm shape. The MAFA was observed to be lowest in the dome region compared with other regions of both ruptured and unruptured aneurysms (Online Supplemental Data). Specifically, the MAFA at the dome (1.9 mL/s, IQR 1.3–3.1, $n = 135$) was significantly lower than the MAFA for the entire aneurysm (2.4 mL/s, IQR 1.7–3.8, $n = 135$) ($P < .001$).

In regression analysis, complex flow patterns (type 3 and 4) were dependently associated with rupture status (OR, 5.57; 95% CI, 2.49–12.45; $P < .001$) in univariate analysis (Online Supplemental Data). Hypertension (OR, 0.42; 95% CI, 0.30–0.54, $P < .001$), bifurcation location (AcomA/ACA/MCA/PcomA/posterior circulation) (OR, 0.17; 95% CI, 0.05–0.29; $P = .005$), and irregular shape (OR, 0.19; 95% CI, 0.05–0.35; $P = .012$) were independently associated with rupture (Online Supplemental Data). Variance inflation factor values for these variables, each below 2.5, indicated no multicollinearity concerns.

Subgroup Analysis

Subgroup analysis of the unruptured aneurysms based on flow patterns revealed that complex flow patterns were significantly more common in unruptured aneurysms associated with daughter sac features ($P = .015$) (Table).

In the subset of 20 aneurysms in which the MAFA within the daughter sac was measured, comprising 14 ruptured and 6 unruptured aneurysms, located in the ICA (7 cases), AcomA (5 cases), PcomA (5 cases), MCA (2 cases), and basilar artery (1 case), the MAFA in the daughter sac (1.5 mL/s, IQR 1.0–2.5) was significantly lower than both the dome region (2.0 mL/s, IQR 1.2–3.1) ($P < .001$) and the entire aneurysm (2.6 mL/s, IQR 1.7–4.0) ($P < .001$) (Online Supplemental Data). Detailed aneurysm characteristics are provided in the Online Supplemental Data.

DISCUSSION

In this prospective cohort study, which included a hemodynamic evaluation by using the AneurysmFlow tool, the key findings are summarized as follows: 1) the complex flow pattern within the aneurysm was observed more frequently in ruptured aneurysms and in unruptured aneurysms associated with daughter sac features; 2) the MAFA at the aneurysmal dome or within any daughter sac is lower than in the remaining areas of the aneurysmal sac, suggesting crucial pathophysiologic changes within the aneurysm wall that are associated with rupture incidence; and 3) hypertension, bifurcation location, and irregular shape are independently associated with aneurysm rupture status.

These results align with other studies by using the CFD method, which have shown that ruptured aneurysms experience more unstable and complex flow profiles compared with unruptured IAs.[22-26] This corroborates the findings of Cebral et al,[31] who indicated that both the DSA-based flow quantification and CFD effectively captured key flow characteristics in approximately 60% of the cases. While previous studies have correlated quantitative hemodynamic evaluation with rupture status,[24-26]

Subgroup analysis of the unruptured aneurysm group based on aneurysm flow patterns

Unruptured Aneurysms	Complex Flow Patterns (Type 3 and 4) (n = 11)	Simple Flow Patterns (Type 1 and 2) (n = 68)	P
Mean aneurysm flow amplitude (MAFA)			
Entire aneurysm, mL/s, median (IQR)	4.0 (3.1–5.3)	3.4 (2.4–4.5)	.520[a]
Neck region, mL/s, median (IQR)	4.6 (3.0–5.2)	3.7 (2.8–4.8)	.563[a]
Inflow region, mL/s, median (IQR)	5.2 (3.7–5.7)	3.5 (2.8–4.4)	.252[a]
Dome region, mL/s, median (IQR)	3.2 (2.1–4.5)	2.8 (1.7–3.9)	.406[a]
Outflow region, mL/s, median (IQR)	3.4 (2.8–4.1)	3.4 (2.2–4.6)	.690[a]
Parent artery, mL/s, median (IQR)	3.8 (3.1–5.0)	3.7 (3.1–4.4)	.760[a]
Clinical characteristics			
Age, year, median (IQR)	51 (44–59)	56 (47–67)	.248[a]
Sex, men, *n* (%)	3 (27.3)	16 (28.1)	.957[b]
Hypertension, *n* (%)	1 (9.1)	3 (5.3)	.624[c]
Smoking, *n* (%)	4 (36.4)	14 (24.6)	.420[b]
Prior history of SAH, *n* (%)	0 (0)	0 (0)	1[c]
Pretreatment with dual antiplatelet therapy, *n* (%)	11 (100)	49 (86.0)	.189[c]
General anesthesia, *n* (%)	0 (0)	5 (8.8)	.311[b]
Anatomic and morphologic characteristics			
ICA location, *n* (%)	7 (63.6)	42 (73.7)	.633[c]
AcomA/ACA/MCA location, *n* (%)	2 (18.2)	3 (5.3)	
PcomA/posterior circulation, *n* (%)	2 (18.2)	12 (21.1)	
Sac width, mm, median (IQR)	5.0 (4.3–9.6)	5.2 (3.7–7.9)	.520[a]
Sac height, mm, median (IQR)	4.9 (4.0–6.5)	5.0 (3.4–6.9)	.763[a]
Neck width, mm, median (IQR)	4.2 (4.0–6.8)	4.1 (3.4–5.4)	.416[a]
Dome to neck ratio, median (IQR)	1.3 (1.1–1.5)	1.3 (1.0–1.5)	.898[a]
Aspect ratio, median (IQR)	1.0 (0.9–1.4)	1.2 (0.9–1.5)	.323[a]
Irregular shape, *n* (%)	9 (81.8)	32 (56.1)	.114[b]
Daughter sac, *n* (%)	8 (72.7)	19 (33.3)	.015[b,d]

[a] P was calculated by using the Student t test.
[b] P was calculated by using the $\chi 2$ test.
[c] P was calculated by using the Mann-Whitney U test.
[d] $P < .05$.

this research did not demonstrate a correlation of MAFA and rupture status. This discrepancy could be explained by several reasons. First, the rate of vasospasm of the parent artery was significantly higher in the ruptured group that is clearly affected on the reduction of MAFA within aneurysm. Second, the reduction of arterial tension under general anesthesia in the ruptured group could be added to the reduction of MAFA both in the parent artery and inside the aneurysm (Online Supplemental Data). Finally, most aneurysms in the ruptured group were small (<7 mm) (75%), which presented some challenges to place the ROIs to accurately measure the MAFA value within the aneurysm.[29]

Contrary to initial expectations, the study found that the MAFA within the dome region or daughter sacs of both ruptured and unruptured aneurysms was the lowest compared with other regions within the aneurysm. This observation is consistent with earlier study by Suzuki and Ohara,[32] which indicated that the wall shear stress in the aneurysm dome tends to be low, despite being the most common rupture site. Furthermore, San Millán Ruíz et al[33] also highlighted that perianeurysmal environment factors influence aneurysm shape and rupture risk. Thus, flow patterns within the aneurysm could predict subsequent morphologic changes, with rupture being more closely linked to aneurysm wall characteristics at the rupture site and the perianeurysmal environment, rather than solely to flow velocities within the aneurysm.

While the flow characteristics assessed by AneurysmFlow tool alone were not strong enough to predict the risk of rupture, clinical, anatomic, and morphologic characteristics still play an important role. Our experiments confirm previous findings showing that hypertension, bifurcation location, and an irregular shape are associated with increased rupture risk.[3-9] Other risk factors, such as smoking or aneurysm size, have been suggested by previous studies as predictors of aneurysm rupture[3-6,34]; however, these findings could not be confirmed by our study. This difference can be explained by the fact that although IAs are more prevalent in the female sex (accounting for 63% in our study), the smoking rate of women in our population was relatively low (only 1.7%).[35] Additionally, small aneurysms (<7 mm) accounted for most in our cohort (75%), which is probably related to the ethnic population.

This study is the first large-scale, prospective examination of aneurysm rupture risk by using the AneurysmFlow tool. Our technique failure rate (8.6%, 12 of 139 patients) was lower than that of Pereira et al[28] (12.5%, 3 of 24 patients). Failures were due to slow contrast medium arrival, excessive field of view, small aneurysm size, or overlap with the parent artery or other branches. Distal aneurysms (eg, AcomA location) also posed challenges due to tortuous anatomy. Ensuring the contrast agent reaches the catheter tip and selecting an optimal field of view (15–22 cm) before imaging is crucial. Aneurysms that are too small, too distal, or overlap significantly with the parent artery or side branches may not be suitable for AneurysmFlow imaging.

We acknowledge several limitations in our research. First, this study had a limited number of patients and was conducted at a single-center. Second, the ruptured aneurysms in our study were all in the acute phase, potentially exhibiting changes in flow and

morphology at the time of rupture compared with their previous unruptured state. This variability complicates the identification of predictive factors for unruptured aneurysms that are going to rupture. Third, this study includes aneurysms originating from various arteries, which is a potential confounding factor in comparing flow characteristics between ruptured and unruptured aneurysms, as the location of the aneurysm may influence flow patterns. The administration of antiplatelet agents and/or heparin before aneurysm flow evaluation procedures poses another potential confounding factor, because it may reduce blood viscosity. Finally, the study utilized a commercial software tool, AneurysmFlow, and these results should be validated by using similar tools from other companies or independent laboratories.

CONCLUSIONS

Complex flow patterns identified on the AneurysmFlow tool are significantly more common in ruptured and unruptured aneurysms associated with daughter sac features. The lowest MAFA in the dome region and daughter sacs suggests specific pathophysiologic changes within the aneurysm wall at the rupture site. Additionally, hypertension, aneurysms located at bifurcations, and irregular aneurysm shapes are independently associated with the rupture risk. A multicenter study with long-term follow-up on unruptured intracranial aneurysms using DSA-based flow evaluation is needed to validate these results.

ACKNOWLEDGMENTS

We would like to thank Dr. Marie Teresa Nawka from the University Hospital of Reims for her valuable contributions in reviewing, enhancing the English style, and providing comments on the manuscript.

Disclosure forms provided by the authors are available with the full text and PDF of this article at www.ajnr.org.

REFERENCES

1. Hop JW, Rinkel GJ, Algra A, et al. **Case-fatality rates and functional outcome after subarachnoid hemorrhage: a systematic review.** *Stroke* 1997;28:660–64 CrossRef Medline
2. McDougall CG, Spetzler RF, Zabramski JM, et al. **The Barrow Ruptured Aneurysm Trial.** *J Neurosurg* 2012;116:135–44 CrossRef Medline
3. Wiebers DO, Whisnant JP, Huston J, 3rd, et al. **Unruptured intracranial aneurysms: natural history, clinical outcome, and risks of surgical and endovascular treatment.** *Lancet* 2003;362:103–10 CrossRef
4. Juvela S, Poussa K, Lehto H, et al. **Natural history of unruptured intracranial aneurysms: a long-term follow-up study.** *Stroke* 2013; 44:2414–21 CrossRef Medline
5. Ishibashi T, Murayama Y, Urashima M, et al. **Unruptured intracranial aneurysms: incidence of rupture and risk factors.** *Stroke* 2009;40:313–16 CrossRef Medline
6. Morita A, Kirino T, Hashi K, et al; UCAS Japan Investigators. **The natural course of unruptured cerebral aneurysms in a Japanese cohort.** *N Engl J Med* 2012;366:2474–82 CrossRef Medline
7. Sonobe M, Yamazaki T, Yonekura M, et al. **Small unruptured intracranial aneurysm verification study: SUAVe study, Japan.** *Stroke* 2010;41:1969–77 CrossRef Medline
8. Sandvei MS, Romundstad PR, Müller TB, et al. **Risk factors for aneurysmal subarachnoid hemorrhage in a prospective population study: the HUNT study in Norway**. *Stroke* 2009;40:1958–62 CrossRef Medline
9. Lee GJ, Eom KS, Lee C, et al. **Rupture of very small intracranial aneurysms: incidence and clinical characteristics.** *J Cerebrovasc Endovasc Neurosurg* 2015;17:217–22 CrossRef Medline
10. Greving JP, Wermer MJ, Brown RD, Jr, et al. **Development of the PHASES score for prediction of risk of rupture of intracranial aneurysms: a pooled analysis of six prospective cohort studies.** *Lancet Neurol* 2014;13:59–66 CrossRef Medline
11. Backes D, Rinkel GJE, Greving JP, et al. **ELAPSS score for prediction of risk of growth of unruptured intracranial aneurysms.** *Neurology* 2017;88:1600–06 CrossRef Medline
12. Etminan N, Brown RD, Jr, Beseoglu K, et al. **The unruptured intracranial aneurysm treatment score: a multidisciplinary consensus.** *Neurology* 2015;85:881–89 CrossRef
13. Sforza DM, Putman CM, Cebral JR. **Hemodynamics of cerebral aneurysms.** *Annu Rev Fluid Mech* 2009;41:91–107 CrossRef Medline
14. Nixon AM, Gunel M, Sumpio BE. **The critical role of hemodynamics in the development of cerebral vascular disease.** *J Neurosurg* 2010;112:1240–53 CrossRef Medline
15. Mantha A, Karmonik C, Benndorf G, et al. **Hemodynamics in a cerebral artery before and after the formation of an aneurysm.** *AJNR Am J Neuroradiol* 2006;27:1113–18 Medline
16. Meng H, Wang Z, Hoi Y, et al. **Complex hemodynamics at the apex of an arterial bifurcation induces vascular remodeling resembling cerebral aneurysm initiation.** *Stroke* 2007;38:1924–31 CrossRef Medline
17. Kulcsár Z, Ugron A, Marosfoi M, et al. **Hemodynamics of cerebral aneurysm initiation: the role of wall shear stress and spatial wall shear stress gradient**. *AJNR Am J Neuroradiol* 2011;32:587–94 CrossRef Medline
18. Boussel L, Rayz V, McCulloch C, et al. **Aneurysm growth occurs at region of low wall shear stress: patient-specific correlation of hemodynamics and growth in a longitudinal study.** *Stroke* 2008; 39:2997–3002 CrossRef Medline
19. Tanoue T, Tateshima S, Villablanca JP, et al. **Wall shear stress distribution inside growing cerebral aneurysm.** *AJNR Am J Neuroradiol* 2011;32:1732–37 CrossRef Medline
20. Cebral JR, Mut F, Weir J, et al. **Quantitative characterization of the hemodynamic environment in ruptured and unruptured brain aneurysms.** *AJNR Am J Neuroradiol* 2011;32:145–51 CrossRef Medline
21. Xiang J, Natarajan SK, Tremmel M, et al. **Hemodynamic-morphologic discriminants for intracranial aneurysm rupture.** *Stroke* 2011;42:144–52 CrossRef Medline
22. Detmer FJ, Chung BJ, Jimenez C, et al. **Associations of hemodynamics, morphology, and patient characteristics with aneurysm rupture stratified by aneurysm location.** *Neuroradiology* 2019;61: 275–84 CrossRef Medline
23. Jing L, Fan J, Wang Y, et al. **Morphologic and hemodynamic analysis in the patients with multiple intracranial aneurysms: ruptured versus unruptured.** *PLoS One* 2015;10:e0132494 CrossRef Medline
24. Takao H, Murayama Y, Otsuka S, et al. **Hemodynamic differences between unruptured and ruptured intracranial aneurysms during observation.** *Stroke* 2012;43:1436–39 CrossRef Medline
25. Fukazawa K, Ishida F, Umeda Y, et al. **Using computational fluid dynamics analysis to characterize local hemodynamic features of middle cerebral artery aneurysm rupture points.** *World Neurosurg* 2015;83:80–86 CrossRef Medline
26. Omodaka S, Sugiyama S, Inoue T, et al. **Local hemodynamics at the rupture point of cerebral aneurysms determined by computational fluid dynamics analysis.** *Cerebrovasc Dis* 2012;34:121–29 CrossRef Medline
27. Bonnefous O, Pereira VM, Ouared R, et al. **Quantification of arterial flow using digital subtraction angiography.** *Med Phys* 2012;39: 6264–75 CrossRef Medline
28. Pereira VM, Bonnefous O, Ouared R, et al. **A DSA-based method using contrast-motion estimation for the assessment of the**

intra-aneurysmal flow changes induced by flow-diverter stents. *AJNR Am J Neuroradiol* 2013;34:808–15 CrossRef Medline
29. Dang Luu V, Xuan Bach T, Huu An N, et al. **Evaluation of hemodynamic alterations after flow diverter placement using the AneurysmFlow™ tool.** *Clin Ter* 2024;175:146–53 CrossRef Medline
30. Ruijters D, Benachour N, Grünhagen T, et al. **How to perform DSA-based cerebral aneurysm flow measurements**. *European Society of Radiology* 2016;2:20
31. Cebral JR, Mut F, Chung BJ, et al. **Understanding angiography-based aneurysm flow fields through comparison with computational fluid dynamics.** *AJNR Am J Neuroradiol* 2017;38:1180–86 CrossRef Medline
32. Suzuki J, Ohara H. **Clinicopathological study of cerebral aneurysms. Origin, rupture, repair, and growth.** *J Neurosurg* 1978;48:505–14 CrossRef Medline
33. San Millán Ruíz D, Yilmaz H, Dehdashti AR, et al. **The perianeurysmal environment: influence on saccular aneurysm shape and rupture**. *AJNR Am J Neuroradiol* 2006;27:504–12 Medline
34. Can A, Castro VM, Ozdemir YH, et al. **Association of intracranial aneurysm rupture with smoking duration, intensity, and cessation.** *Neurology* 2017;89:1408–15 CrossRef Medline
35. World Health Organization. **Tobacco [Internet]** 2023. Accessed May 19, 2024. https://www.who.int/vietnam/news/commentaries/detail/women-and-tobacco-in-viet-nam–the-hidden-threat